Polarization Reversal and Second-Order Optical Nonlinearity of Uniaxially Drawn Aliphatic Polyurea

Naoto Tsutsumi,* Yasuyoshi Okabe, and Wataru Sakai

Department of Polymer Science & Engineering, Kyoto Institute of Technology, Matsugasaki, Sakyo, Kyoto 606-8585, Japan

Received November 2, 1998; Revised Manuscript Received March 5, 1999

ABSTRACT: Molecular orientation, polarization reversal, and second-order optical nonlinearity have been studied for the uniaxially drawn aliphatic polyurea films. Aliphatic polyurea (PU7) was synthesized from 1,7-diaminoheptane and urea via a condensation reaction. Melt-pressed films were uniaxially drawn by ratios of 1.4, 1.8, 2.0, 2.5, and 2.8. Clear polarization reversal can be measured when the samples are subjected to the sinusoidal electric field at room temperature and at 60 °C which is above the glass transition temperature. Remanent polarization is larger for the sample poled at 60 °C than for the sample poled at room temperature. Average molecular angles, $\overline{\Phi_X}$, $\overline{\Phi_Y}$, and $\overline{\Phi_Z}$, in three laboratory frames are evaluated from the refractive indices. $\overline{\Phi_X}$ decreases and $\overline{\Phi_Y}$ and $\overline{\Phi_Z}$ increase with increasing draw ratio. Dependence of second-order harmonic (SH) intensity on incidence angle, i.e., the Maker fringe pattern, could be fitted using two independent tensor components, d_{33} and d_{31}, for undrawn and poled film and three independent tensor components, d_{33}, d_{32}, and d_{31} for the poled films drawn to a ratio of 1.4 and five independent tensor components, d_{33}, d_{32}, d_{31}, d_{15}, and d_{24}, for the poled films drawn to higher ratios of 2.0 and 2.5. For films drawn to the higher ratios of 2.0 and 2.5, Kleinman symmetry was not satisfied: $d_{31} \neq d_{15}$ and $d_{32} \neq d_{24}$. Increase of the draw ratio gave rise to the large increase of the tensor components d_{33} and d_{31}, the moderate increase of d_{24}, and the gradual decrease of d_{15} and d_{32}. The large linear dependence of electrooptic response on electric field is ascribed to the linear electrooptic (Pockels) effect as well as the piezoelectric response.

Introduction

The first report regarding the second-order optical nonlinearity in ferroelectric polymers had been made for poly(vinylidene fluoride) (PVDF) films in the 1970s.[1,2] Second harmonic generation (SHG) of the ferroelectric copolymer of vinylidene fluoride and trifluoroethylene (P(VDF−TrFE)) was also studied,[3−5] and the proportionality between the d_{33} value and P_r was reported.[4] Furthermore second-order optical nonlinearity was measured for a blend of P(VDF−TrFE) with poly(methyl methacrylate) (PMMA) (P(VDF−TrFE)/PMMA blends)[6] and nonlinear optical (NLO) dye dispersed PVDF/PMMA blends.[7]

The second-order optical nonlinearity in drawn and poled Nylon 11, which shows clear ferroelectric polarization reversal,[8,9] has been investigated by Tsutsumi et al.[10,11] The Maker fringe pattern could be precisely fitted using five independent nonvanishing tensor components, d_{33}, d_{32}, d_{31}, d_{15}, and d_{24}. Kleinman symmetry was not satisfied: $d_{31} \neq d_{15}$ and $d_{32} \neq d_{24}$. The tensor components d_{33}, d_{31}, d_{15}, and d_{24} increase with increasing remanent polarization, whereas the value of d_{32} is negligibly small irrespective of the intensity of the remanent polarization. Using an oriented gas model, tensor components of microscopic first-order hyperpolarizability, β_{zxx}, β_{zyy},, β_{zzz}, β_{xxz}, and β_{yyz} can be determined from the observed d coefficients. The tensor component β_{zzz} is the largest, and β_{zxx} has a negative sign for all samples.

In the case of Nylon 11, the amide (−NHCO−) moiety itself and noncentrosymmetric alignment of amide groups are significantly responsibile for the ferroelectric response including polarization reversal and second-order optical nonlinearity. In analogy to odd nylons, e.g. Nylon 11, an odd aliphatic polyurea with the −NHCONH− moiety is expected to exhibit polarization reversal and second-order optical nonlinearity. In this study, we have investigated molecular orientation, polarization reversal, and second-order optical nonlinearity for the drawn and poled aliphatic polyurea. The effects of drawing and poling on these properties have been discussed.

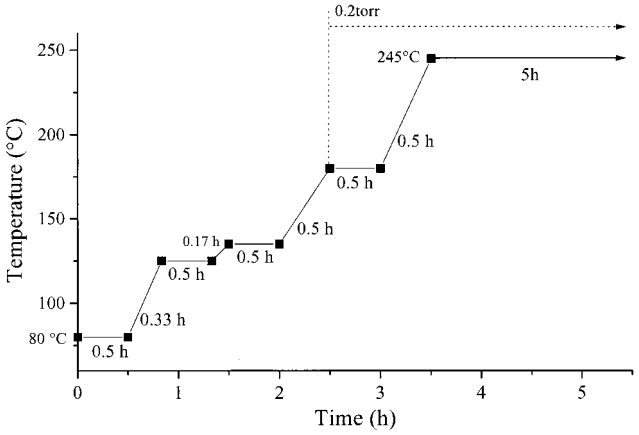

Figure 1. Temperature−time scheme for the polymerization process.

Experimental Section

Sample Preparation. Aliphatic polyurea (PU7) was synthesized from 1,7-diaminoheptane (1,7-DAH) and urea via a condensation reaction. A mixture of 1,7-DAH (2.76 g, 0.0212 mol) and urea (1.26 g, 0.0212 mol) was heated stepwise along the temperature−time scheme shown in Figure 1. For the final

* To whom correspondence should be addressed.

10.1021/ma981704k CCC: $18.00
Published on Web 04/24/1999

6 h, the reaction mixture was in vacuo to remove the generated ammonia gas. PU7 film was melt-pressed between Upilex polyimide films at 260 °C on a heated press to thickness of ca. 40−60 μm. The molten films were quenched into liquid nitrogen. Neat PU7 films were drawn at 1.4, 1.8, 2.0, 2.5, and 2.8 ratios at room temperature to a thickness of 25−50 μm.

Electrical and Optical Measurements. For the poling process, 0.05 Hz sinusoidal voltage was applied for 1 h at room temperature to the aluminum electrodes, which had been evaporated onto opposing surfaces of the films, in a 3 M inert liquid, Fluorinert FC40. The poling current was monitored during application of the voltage and was used to calculate the remanent polarization, allowing for impedance losses.[12,13] Aluminum electrodes were removed by immersing them in 10 wt % sodium hydroxide solution for a few minutes.

A prism coupling method was employed to measure the refractive indices of PU7 films. Laser sources are a polarized He−Ne laser (632.8 nm) and a laser diode (830 nm). The prism of TaFD21 (HOYA Glass) with high refractive index (1.92588 at 632.8 nm) and film was coupled with an air gap. The critical angle at which a complete reflection changes to partial reflection, i.e., the part of the light penetrates into the film bulk, was measured to determine the refractive indices, since the film thickness is approximately 30 μm. Laser intensity drop due to the partial light penetration into film bulk at critical angle is very sharp, and indeed the experimental error of each measurement is considered to be within ±0.0001. Thus the refractive index measured using this method has the accuracy to the fourth decimal place. Ultraviolet−visible spectra of the films were measured in transmission on a UV−vis spectrometer after the aluminum electrodes were removed.

A transmission-modulated technique was used to evaluate the electrooptic response. The original simple reflection technique[14] is modified to permit transmission measurement. The light source is a linear polarized He−Ne laser (632.8 nm) with 0.5 mW. A linear polarizer placed before the sample film provides linearly polarized light at 45° with respect to the plane of incidence. This results in equal components of *s*- and *p*-polarizations. The sample film was sandwiched between two glass plates coated with transparent indium tin oxide electrodes. The sample plane was rotated by 45° with respect to normal incidence. The transmitted light beam propagates through a Babinet compensator analyzer whose polarization linearly polarized light at 45° with respect to the plane of incidence. The electrooptic effect of the sample film was measured from the change of He−Ne laser intensity when the sample film was subjected to a sinusoidal voltage of 1 kHz with an amplitude between 100 and 500 V. The responses at 1 and 2 kHz were recorded using a lock-in amplifier.

Second Harmonic Generation Measurements. The Maker fringe method[15,16] was employed to measure the generated second harmonic (SH) intensity for poled films. Laser source is a Continuum model Surelite-10 Q-switched Nd:YAG pulse laser with 1064 nm *p*-polarized fundamental beam (320 mJ maximum energy, 7 ns pulse width, and 10 Hz repeating rate). The generated SH wave was detected by a photomultiplier. The SH signal averaged on a gated integrator and boxcar averager module was transferred to a microcomputer through a computer interface module. The detailed experimental procedure is described in refs 6 and 7.

Characterization. Wide-angle X-ray scattering (WAXS) patterns of the films were measured on a X-ray diffractometer with nickel-filtered Cu Kα radiation. Diffrential scanning calorimetry (DSC) was carried out at a heating rate of 10 °C/min in a nitrogen atmosphere.

Results and Discussion

Polymer Structure. Figure 2 shows WAXS profiles for melt-quenched and drawn sample films. WAXS profiles show that the melt-quenched and drawn sample has its intensity maximum at an angle (2θ) around 21.0°. These profiles do not give rise to the significant change in crystallinity and crystallite size upon drawing.

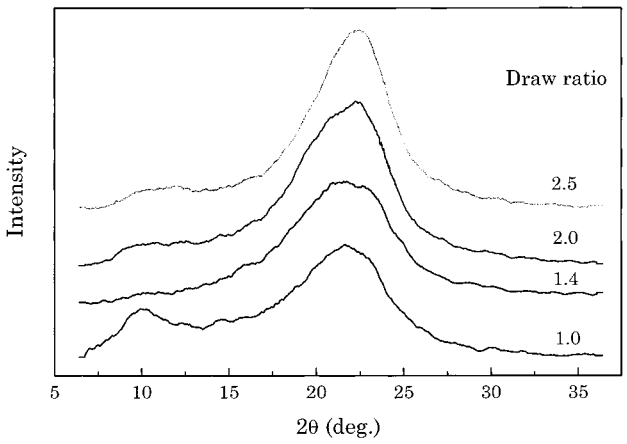

Figure 2. WAXS pattern for melt-quenched and drawn films.

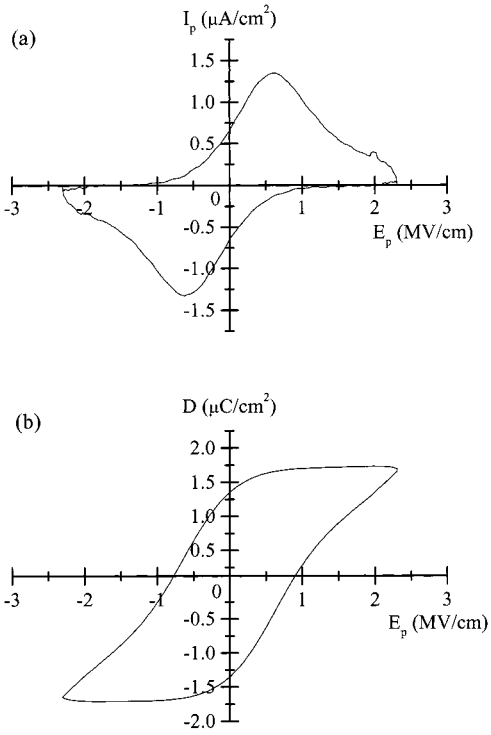

Figure 3. Polarization current (a) and polarization charge (time integral of polarization curent, b) for PU7 film uniaxially drawn to ratio of 2.5 at 60 °C.

DSC thermogram of a melt-quenched PU7 film shows a clear endothermic transition due to the glass transition at 62 °C, an exothermic peak due to cold crystallization at 105 °C, and an endothermic peak due to crystallite melting at 241 °C. In the DSC thermogram, the melting enthalpy due to the melting of crystallite at 241 °C is not changed by drawing and is almost the same as that for melt-quenched sample film. DSC results also suggest that drawing does not significantly change the crystalline morphology.

Polarization Current and Polarization Charge. Figure 3 shows the polarization current and its time integral (polarization charge) for the drawn film (draw ratio of 2.5) as a function of sinusoidal electric field with maximum field (E_{max} = 2.3 MV/cm) at 60 °C. Current flows on the external circuit are the summation of the current due to the polarization, capacitance, and conductivity,[13] i.e.,

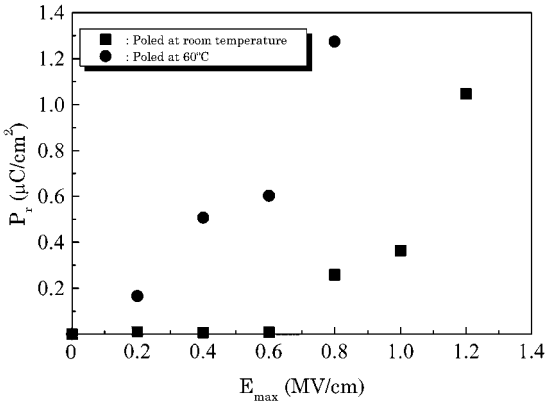

Figure 4. Plots of P_r as a function of E_{max}. Filled square: Poled at room temperature. Filled circle: Poled at 60 °C. All films are undrawn samples.

$$J = J_D + J_\rho = \frac{dP}{dt} + \epsilon\epsilon_0 \frac{dE}{dt} + \frac{E}{\rho} \quad (1)$$

where J the is poling current, J_D is the displacement current, J_ρ is the conduction current, ϵ is the relative permittivity, ϵ_0 is the permittivity of vacuum, P is the polarization, E is the applied electric field, and ρ is the resistivity. The polarization current in Figure 3 is the poling current reduced by the terms due to capacitance and conductivity. In the polarization charge profile, the remanent polarization (P_r) is the value of polarization at zero applied field and the coercive field (E_c) is the applied field at zero polarization after the last cycle of poling.

Figure 4 shows the dependence of P_r on the maximum applied electric field (E_{max}) when undrawn sample films are sinusoidally poled at room temperature and at 60 °C which is close to the glass transition temperature of the matrix. P_r value obtained at 60 °C is larger than that obtained at room temperature at the same maximum applied field. Poling at 60 °C gave the larger remanent polarization at lower maximum applied field. The polarization reversal of the present polyurea sample is ascribed to both the alignment of the urea dipole moments in the crystalline region and in the amorphous region assisted by the segmental molecular motion above glass transition temperature. This result is contrast to the fact that the polarization reversal in ferroelectric Nylon 11 is attributed to the crystallite dipoles.[10,11] Absolute values of P_r for PU7 is 0.5−1.5 μC/cm^2 which is smaller than the corresponding ones, 4−6 μC/cm^2 for Nylon 11. From the MOPAC PM3 molecular dynamics calculations, both dipole moments are almost comparable. Then, the difference in P_r values between PU7 and Nylon 11 may be ascribed to the sample histories. The smaller remanent polarization is significantly related to the smaller SH coefficients for PU7 films (vide infra).

Refractive Indices. The refractive indices (n) for transverse electric field (TE) and transverse magnetic field (TM) modes are measured using a prism coupling method at wavelengths of 632.8 and 830 nm. TM mode measurement provides the n value along the direction of film thickness, and TE mode measurement gives the n value in the plane of film. n values at wavelengths of 632.8 and 830 nm were listed for the unpoled (A) and poled (B) polymer films in Table 1. Here n_X, n_Y, and n_Z are n values along the drawing direction, perpendicular to the drawing direction in the plane of film, and along the poling direction parallel to the film thickness direction, respectively. Wavelength dispersion of n, $n_f(\lambda)$, can be fitted to a one-oscillator Sellmeier dispersion formula

$$n_f^2(\lambda) - 1 = \frac{q}{1/\lambda_0^2 - 1/\lambda^2} + A \quad (2)$$

where λ_0 is the absorption wavelength of the dominant oscillator, q is a measure for the oscillator strength, and A is a constant containing the sum of all the other oscillators. PU7 film has the first absorption maximum at 218 nm due to the n−π* transition of the carbonyl group in urea bonding. Refractive indices at 532 and 1064 nm obtained from the predicted plots of eq 2 with $\lambda_0 = 218$ nm are also listed in Table 1, which were used for determination of SH coefficients.

Figure 5 shows the wavelength dependence of n, n_X, n_Y, and n_Z, before and after poling, for the samples with draw ratios of 1.0 (a), 1.4 (b), 2.0 (c), and 2.5 (d). The poling condition was as follows: sinusiodal poling with maximum field of 2.0 MV/cm ($P_r = 1-1.5$ μC/cm^2). For drawn samples, large anisotropies of $n_X > n_Y > n_Z$ was measured, and the anisotropy originates from the alignment of polymer chain along the drawing direction. The largest refractive index, n_X, is obtained along the drawing direction, and the smallest one, n_Z, is obtained in the direction of film thickness, perpendicular to the surface plane of the films.

Effect of Drawing and Poling on Molecular Orientation. Anisotropic orientation of molecules can be estimated from the three-dimensional refractive indices, n_X, n_Y, and n_Z. Each refractive index, n_X, n_Y, and n_Z, can be expressed as[17,18]

$$n_i = (n_{\parallel} - n_{\perp})\overline{\cos^2 \Phi_i} + n_{\perp} \quad (i = X, Y, Z) \quad (3)$$

$$\overline{\cos^2 \Phi_X} + \overline{\cos^2 \Phi_Y} + \overline{\cos^2 \Phi_Z} = 1 \quad (4)$$

where $n_{\parallel}$ and $n_{\perp}$ are the intrinsic refractive indices parallel and perpendicular to molecular chain axis, respectively, $(n_{\parallel} - n_{\perp})$ is the intrinsic birefringence, and molecular angles Φ_X, Φ_Y, and Φ_Z are the angles between molecular axis in the chain direction and laboratory frame, X, Y, and Z, respectively. The X-axis is parallel to the drawing direction, the Y-axis is perpendicular to the X-axis in the plane of the film, and the Z-axis is the direction to film thickness (poling direction). The quantity $\overline{\cos^2 \Phi}$ is defined as

$$\overline{\cos^2 \Phi} = \frac{\int_0^{\pi/2} G(\Phi) \cos^2 \Phi \sin \Phi \, d\Phi}{\int_0^{\pi/2} G(\Phi) \sin \Phi \, d\Phi} \quad (5)$$

$G(\Phi)$ is the orientational distribution function, which is usally defined by Gaussian or Lorentzian distribution functions. Average molecular angles $\overline{\Phi_X}$, $\overline{\Phi_Y}$, and $\overline{\Phi_Z}$ can be given by

$$\overline{\Phi} = \frac{\int_0^{\pi/2} G(\Phi) \Phi \sin \Phi \, d\Phi}{\int_0^{\pi/2} G(\Phi) \sin \Phi \, d\Phi} \quad (6)$$

Average molecular angles $\overline{\Phi_X}$, $\overline{\Phi_Y}$, and $\overline{\Phi_Z}$, in three directions (X, Y, and Z) can be evaluated from the

Table 1. *n* Values at Wavelengths of 632.8 and 830 nm Measured and Those at 532 and 1064 nm Predicted by Eq 2

(A) Unpoled Sample

(a) Draw Ratio = 1.0 (Undrawn)

	wavelength (nm)			
	632.8	830	532	1064
n_X	1.5307	1.5226	1.5396	1.5185
n_Y	1.5307	1.5226	1.5396	1.5185
n_Z	1.5301	1.5224	1.5387	1.5184

(b) Draw Ratio = 1.4

	wavelength (nm)			
	632.8	830	532	1064
n_X	1.5404	1.5330	1.5486	1.5292
n_Y	1.5322	1.5249	1.5404	1.5213
n_Z	1.5294	1.5226	1.5369	1.5192

(c) Draw Ratio = 2.0

	wavelength (nm)			
	632.8	830	532	1064
n_X	1.5470	1.5393	1.5557	1.5355
n_Y	1.5268	1.5216	1.5326	1.5190
n_Z	1.5244	1.5185	1.5311	1.5156

(d) Draw Ratio = 2.5

	wavelength (nm)			
	632.8	830	532	1064
n_X	1.5575	1.5517	1.5641	1.5489
n_Y	1.5286	1.5254	1.5322	1.5238
n_Z	1.5197	1.5133	1.5269	1.5100

(B) Poled Sample

(a) Draw Ratio = 1.0

	wavelength (nm)			
	632.8	830	532	1064
n_X	1.5373	1.5310	1.5444	1.5278
n_Y	1.5373	1.5310	1.5444	1.5278
n_Z	1.5361	1.5290	1.5439	1.5254

(b) Draw Ratio = 1.4

	wavelength (nm)			
	632.8	830	532	1064
n_X	1.5465	1.5393	1.5544	1.5357
n_Y	1.5396	1.5353	1.5444	1.5332
n_Z	1.5389	1.5348	1.5434	1.5328

(c) Draw Ratio = 2.0

	wavelength (nm)			
	632.8	830	532	1064
n_X	1.5535	1.5443	1.5636	1.5397
n_Y	1.5356	1.5328	1.5386	1.5314
n_Z	1.5320	1.5272	1.5372	1.5248

(d) Draw Ratio = 2.5

	wavelength (nm)			
	632.8	830	532	1064
n_X	1.5605	1.5536	1.5680	1.5503
n_Y	1.5294	1.5252	1.5340	1.5231
n_Z	1.5273	1.5193	1.5362	1.5153

relation between $\overline{\Phi}$ and $\overline{\cos^2\Phi}$. Figure 6 shows the dependence of $\overline{\Phi_X}$, $\overline{\Phi_Y}$, and $\overline{\Phi_Z}$ on draw ratio. These average molecular angles are evaluated using eqs 3−6 with refractive indices at 632.8 nm in Table 1 and ($n_{\|} - n_{\perp}$) = 0.055.[19] Figure 6 shows that the degree of orientation to *X*-axis increases as the draw ratio increases, and if the molecular chains completely extend along the *X*-axis, $\overline{\cos^2\Phi_X} = 1$ and $\overline{\cos^2\Phi_Y} = \overline{\cos^2\Phi_Z} = 0$ ($\overline{\Phi_X} = 0°$ and $\overline{\Phi_Y} = \overline{\Phi_Z} = 90°$) are obtained.

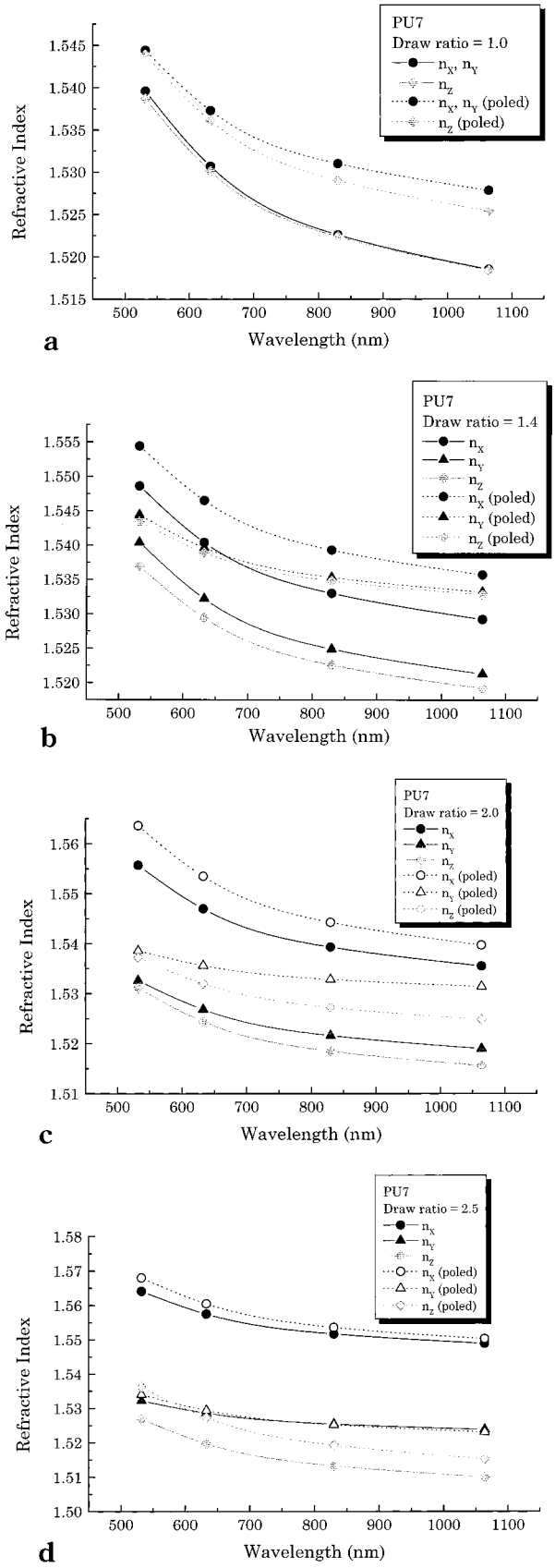

Figure 5. Dependence of refractive index on wavelength for unpoled film (filled symbol) and poled film (open symbol) with various draw ratio of 1.0 (a), 1.4 (b), 2.0 (c) and 2.5 (d).

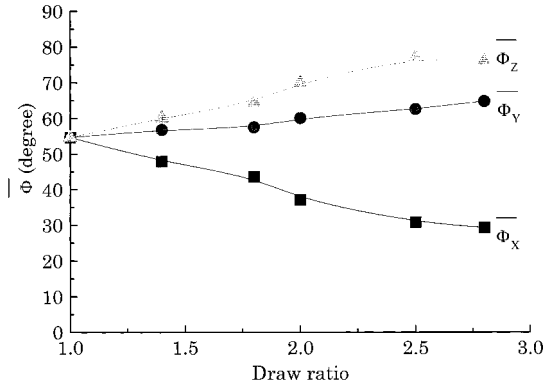

Figure 6. Plots of average molecular angles, $\overline{\Phi_X}$, $\overline{\Phi_Y}$, and $\overline{\Phi_Z}$ as a function of draw ratio.

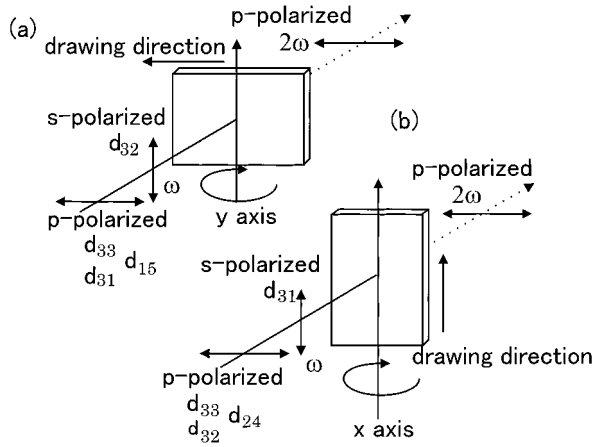

Figure 7. Schematic configuration of Maker fringe SH measurements. Double-ended arrows represent the polarization of the wave.

Second-Order Optical Nonlinearity. The poling process induces a polar axis in the poled polymer film. The axis is essentially an infinite-fold rotational axis with an infinite number of mirror planes.[20] Undrawn and poled polymers belong to the ∞mm point group. Drawn and poled polymers belong to the $mm2$ point group, where the symmetry operations include a 2-fold axis along the film normal direction and two mirror planes perpendicular to each other. In both cases, nonlinear polarization P_{NL} is given by

$$P_{\mathrm{NL}} = \begin{pmatrix} 0 & 0 & 0 & 0 & d_{15} & 0 \\ 0 & 0 & 0 & d_{24} & 0 & 0 \\ d_{31} & d_{32} & d_{33} & 0 & 0 & 0 \end{pmatrix} \begin{pmatrix} E_1^2 \\ E_2^2 \\ E_3^2 \\ 2E_2E_3 \\ 2E_1E_3 \\ 2E_1E_2 \end{pmatrix} \qquad (7)$$

where there are five nonvanishing d coefficients.

Maker fringe analysis[15,16] was employed to determine these SH coefficients. The same schematic configuration of SH measurements as in the case of Nylon 11[11] was used, which is illustrated in Figure 7. The measurements were made relative to a Y-cut quartz plate ($d_{11} = 1.2 \times 10^{-9}$ esu (=0.5 pm/V)). In this technique, a plane sample was rotated in the path of a fundamental beam of wavelength of 1064 nm from a Q-switched Nd:YAG pulse laser.

Maker fringe patterns for an undrawn sample can be characterized by two independent d coefficients, d_{33} and $d_{31}(= d_{32} = d_{15} = d_{24})$, whereas those for the drawn sample are characterized by three independent d coefficients, d_{33}, $d_{31}(=d_{15})$, and d_{32} $(=d_{24})$, or five independent d coefficients, d_{33}, d_{31}, d_{32}, d_{15}, and d_{24}. Typical Maker fringe patterns for the drawn and poled sample film (draw ratio of 2.0) with $P_r = 1.3\ \mu$C/cm^2 are shown in Figure 8. The solid curve in Figure 8 is the theoretical fitting with $n_X{}^{\omega} = 1.5397$, $n_X{}^{2\omega} = 1.5636$, $n_Y{}^{\omega} = 1.5314$, $n_Y{}^{2\omega} = 1.5386$, $n_Z{}^{\omega} = 1.5248$, and $n_Z{}^{2\omega} = 1.5372$. Theoretical plots in Figure 8a give $d_{33} = 0.082$ pm/V, $d_{31} = 0.053$ pm/V, and $d_{15} = 0.0016$ pm/V and those in Figure 8b give $d_{33} = 0.082$ pm/V, $d_{24} = 0.021$ pm/V, and $d_{32} = 0.0062$ pm/V. The details of the theoretical fitting procedure is discussed in ref 11. It is noted that SH intensity for the X-axis rotation sp including the tensor component d_{31} is larger than that for the Y-axis rotation pp including the components of d_{31}, d_{33}, and d_{15}. d Values are plotted against maximum electric field on poling in Figure 9 for the samples with draw ratios 2.0 (a) and 2.5 (b). All d values significantly increase with increasing maximum electric field. The d value for the present PU7 is smaller than those obtained in Nylon 11.[11] The smaller d values in PU7 are consistent with the fact that the remanent polarization in PU7 is smaller than that in Nylon 11 mentioned above. The total number of the dipoles contributing to the nonlinear optical polarization as well as the remanent polarization is smaller than those in Nylon 11.

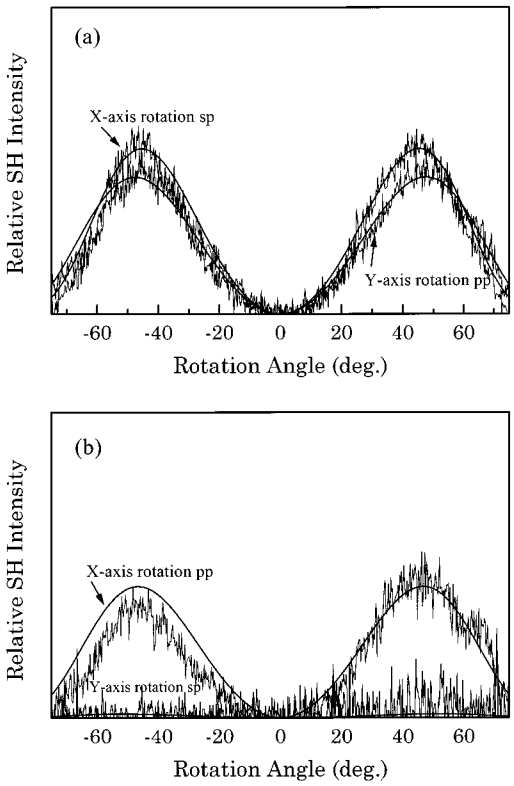

Figure 8. Typical Maker fringe patterns of the drawn and poled films. Solid curve is the theoretical fitting using eq 6 with $n_X{}^{\omega} = 1.5397$, $n_X{}^{2\omega} = 1.5636$, $n_Y{}^{\omega} = 1.5314$, $n_Y{}^{2\omega} = 1.5386$, $n_Z{}^{\omega} = 1.5248$, and $n_Z{}^{2\omega} = 1.5372$. Theoretical plots in part a give $d_{33} = 0.082$ pm/V, $d_{31} = 0.053$ pm/V, and $d_{15} = 0.0016$ pm/V and those in part b give $d_{33} = 0.082$ pm/V, $d_{24} = 0.021$ pm/V, and $d_{32} = 0.0062$ pm/V.

The dependence of d coefficients on draw ratio is shown in Figure 10. The poling field is 1.5 MV/cm. Fringe patterns for the films with a draw ratio of 1.4 can be characterized by three independent d values, d_{33},

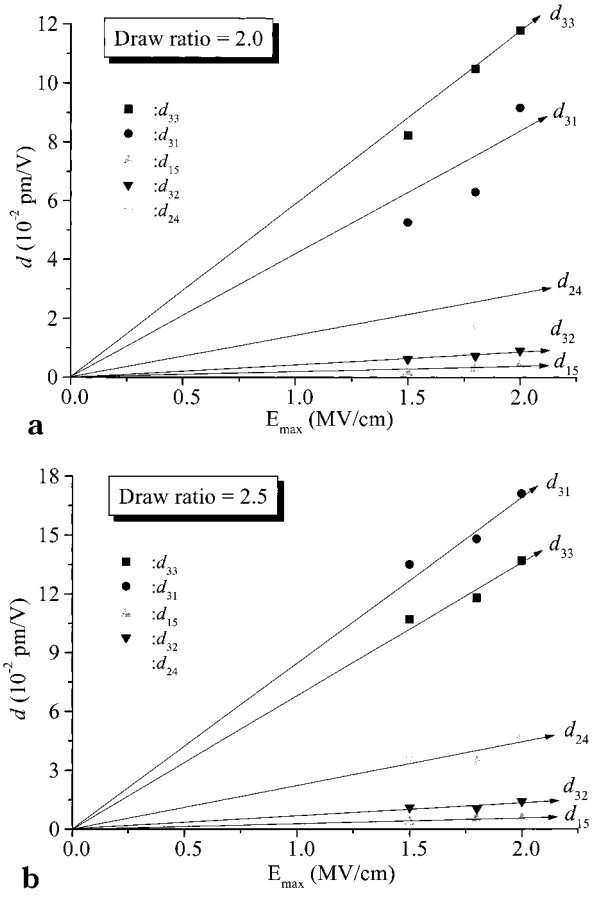

Figure 9. Plots of SH coefficients d_{33}, d_{32}, d_{31}, d_{15}, and d_{24} vs E_{max} for the samples with various draw ratio of 2.0 (a) and 2.5 (b).

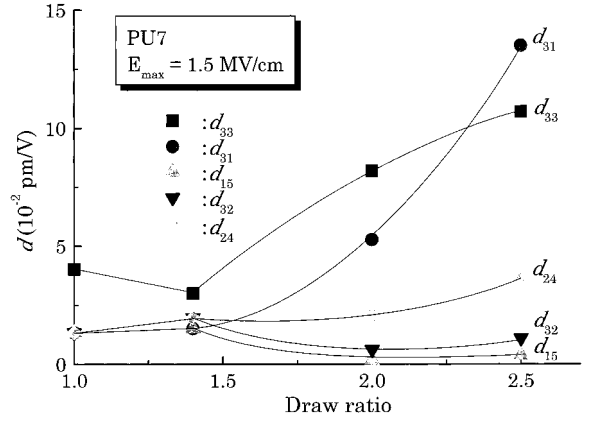

Figure 10. Plots of SH coefficients d_{33}, d_{32}, d_{31}, d_{15}, and d_{24} vs draw ratio.

d_{31}, and d_{32}, instead of two independent d coefficients, d_{33} and d_{31}, for the undrawn and poled PU7 films. Watanabe et al.[21] reported that d_{31} increases and d_{32} and d_{33} decrease with increasing draw ratio up to 1.3 for the main chain polymer including two-dimensional charge transfer (2-D CT) molecules, whereas the d_{31}/d_{32} ratios is independent of the draw ratio for the side chain polymer containing one-dimensional CT molecules. Fringe patterns for the films with higher draw ratios of 2.0 and 2.5 were characterized by five independent d coefficients, d_{33}, d_{31}, d_{32}, d_{15}, and d_{24}. With increasing draw ratios, d_{33} increases and d_{31} extremely increases, d_{24} moderately increases, and d_{15} and d_{32} gradually decrease. It is noted that the d_{31} value at the draw ratio of 2.5 exceeds the d_{33} value and the relation $d_{31} \geq d_{33} > d_{24} > d_{32} > d_{15}$ is obtained.

The macroscopic nonlinear optical coefficient d_{IJK} is expressed in terms of molecular second-order susceptibility b_{IJK},

$$d_{IJK} = N f_I^{2\omega} f_J^{\omega} f_K^{\omega} b_{IJK} \tag{8}$$

where N is the number density of noncentrosymmetric molecules per unit volume, and $f_I^{2\omega}$, f_J^{ω}, and f_K^{ω} are Lorentz−Lorenz local field factors

$$f_I^{\omega} = \frac{(n_I^{\omega})^2 + 2}{3} \tag{9}$$

where n_I^{ω} is the refractive index in direction I.

Theoretical treatment between molecular second-order susceptibility b_{IJK} and microscopic molecular hyperpolarizability β_{ijk} was formerly given by Watanabe et al.[21] and details are shown in ref 11.

$$b_{33} = \frac{\mu E}{15kT}(2\langle\cos^2\alpha\rangle\beta_{zxx} + 2\langle\sin^2\alpha\rangle\beta_{zyy} + 3\beta_{zzz} + 4\langle\cos^2\alpha\rangle\beta_{xxz} + 4\langle\sin^2\alpha\rangle\beta_{yyz}) \tag{10}$$

$$b_{31} = \frac{\mu E}{15kT}[(3\langle\cos^2\alpha\rangle\langle\cos^2\phi\rangle + 5\langle\sin^2\alpha\rangle\langle\sin^2\phi\rangle)\beta_{zxx} + (3\langle\sin^2\alpha\rangle\langle\cos^2\phi\rangle + 5\langle\cos^2\alpha\rangle\langle\sin^2\phi\rangle)\beta_{zyy} + 2\langle\cos^2\phi\rangle\beta_{zzz} - 4\langle\cos^2\alpha\rangle\langle\cos^2\phi\rangle\beta_{xxz} - 4\langle\sin^2\alpha\rangle\langle\cos^2\phi\rangle\beta_{yyz}] \tag{11}$$

$$b_{32} = \frac{\mu E}{15kT}[(3\langle\cos^2\alpha\rangle\langle\sin^2\phi\rangle + 5\langle\sin^2\alpha\rangle\langle\cos^2\phi\rangle)\beta_{zxx} + (3\langle\sin^2\alpha\rangle\langle\sin^2\phi\rangle + 5\langle\cos^2\alpha\rangle\langle\cos^2\phi\rangle)\beta_{zyy} + 2\langle\sin^2\phi\rangle\beta_{zzz} - 4\langle\cos^2\alpha\rangle\langle\sin^2\phi\rangle\beta_{xxz} - 4\langle\sin^2\alpha\rangle\langle\sin^2\phi\rangle\beta_{yyz}] \tag{12}$$

$$b_{15} = \frac{\mu E}{15kT}[-2\langle\cos^2\alpha\rangle\langle\cos^2\phi\rangle\beta_{zxx} - 2\langle\sin^2\alpha\rangle\langle\cos^2\phi\rangle\beta_{zyy} + 2\langle\cos^2\alpha\rangle\beta_{zzz} + (\langle\cos^2\alpha\rangle\langle\cos^2\phi\rangle + 5\langle\sin^2\alpha\rangle\langle\sin^2\phi\rangle)\beta_{xxz} + (\langle\sin^2\alpha\rangle\langle\cos^2\phi\rangle + 5\langle\cos^2\alpha\rangle\langle\sin^2\phi\rangle)\beta_{yyz}] \tag{13}$$

$$b_{24} = \frac{\mu E}{15kT}[-2\langle\cos^2\alpha\rangle\langle\sin^2\phi\rangle\beta_{zxx} - 2\langle\sin^2\alpha\rangle\langle\sin^2\phi\rangle\beta_{zyy} + 2\langle\sin^2\phi\rangle\beta_{zzz} + (\langle\cos^2\alpha\rangle\langle\sin^2\phi\rangle + 5\langle\sin^2\alpha\rangle\langle\cos^2\phi\rangle)\beta_{xxz} + (\langle\sin^2\alpha\rangle\langle\sin^2\phi\rangle + 5\langle\cos^2\alpha\rangle\langle\cos^2\phi\rangle)\beta_{yyz}] \tag{14}$$

where ϕ and α are Euler angles introduced to transform the laboratory frame (X, Y and Z) to the molecular frame (x, y and z). Five independent nonlinear optical coefficients d_{33}, d_{31}, d_{32}, d_{15}, and d_{24} can be combined with tensor components of microscopic hyperpolarizability using eqs 10−14 with eq 8, respectively.

As reported for Nylon 11,[11] $\langle\cos^2\phi\rangle$ (or $\langle\cos^2\alpha\rangle$) for the samples with draw ratios of 2.0 and 2.5 are observed to

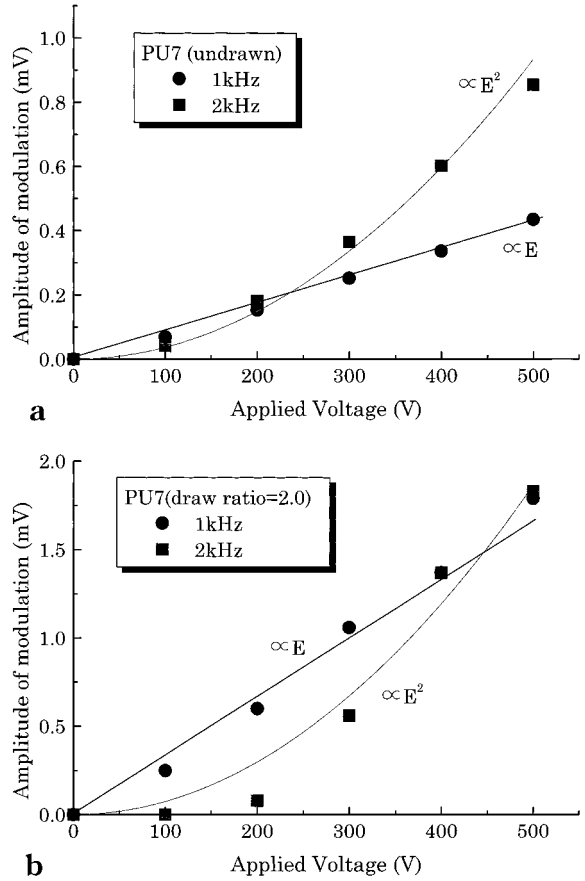

Figure 11. Electrooptic response of undrawn and drawn samples: (a) undrawn samples; (b) drawn samples with a draw ratio of 2.0. Samples were poled with $E_{max} = 1.5$ MV/cm at 60 °C.

be 0.85 and 1.00, respectively. Thus, five independent d coefficients, d_{33}, d_{31}, d_{32}, d_{15}, and d_{24}, at the draw ratio of 2.5 are characterized by five independent microscopic molecular hyperpolarizabilities β_{zzz}, β_{zxx}, β_{xxz}, β_{zyy}, and β_{yyz} using the above equations. In this case, the relation $\beta_{zxx} \approx \beta_{zzz} > \beta_{yyz} > \beta_{zyy} > \beta_{xxz} \approx 0$ is satisfied. It is supposed that, for a highly drawn PU7 film, the dipoles align along the orientational chain direction with the assistance of strong hydrogen bonding. Analysis of Maker fringe patterns for the drawn and poled Nylon 11 also gave five independent d coefficients, d_{33}, d_{31}, d_{32}, d_{15}, and d_{24}.[11] In that case, the relation of $d_{33} \simeq d_{15} > d_{31} \simeq d_{24} \gg d_{32}$ was characterized by five independent microscopic molecular hyperpolarizabilities with the relation $\beta_{zzz} > \beta_{yyz} > \beta_{xxz} > \beta_{zyy} \approx 0$ and β_{zxx} with negaive sign. In both case of Nylon 11 and the present PU7, the large anisotropy induced at a draw ratio above 2.0 significantly breaks the Kleinman symmetry: $d_{31} \neq d_{15}$ and $d_{32} \neq d_{24}$.

Electrooptic Response. Figure 11 shows the electrooptic response for the poled undrawn and drawn samples. As described in the Experimental Section, the eletro-optic effect of the sample film was evaluated from the change of laser intensity with equal components of *p*- and *s*-polarizations when the sample film was subjected to sinsoidal voltage at 1 kHz. Responses at 1 and 2 kHz were observed for both samples. The response at 1 kHz has a linear relationship with the applied voltage and that at 2 kHz has a quadratic relationship with the applied voltage. No significant response at 3 kHz was observed. The linear response includes the linear electrooptic (Pockels) as well as the piezoelectric responses.

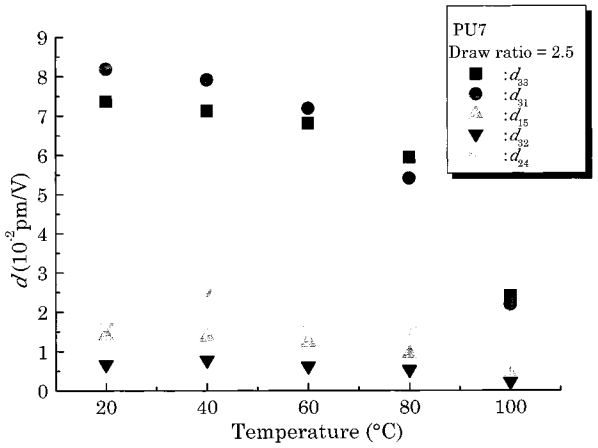

Figure 12. Dependence of SH coefficients d_{33}, d_{32}, d_{31}, d_{15}, and d_{24} on annealing temperature. Annealing time: 1 h. Sample with draw ratio of 2.5 was poled sinusoidally with $E_{max} = 1.5$ MV/cm.

Quadratic response is ascribed to the electrostriction effect. For undrawn sample film, electrooptic coefficient r_{33} for undrawn sample can be measured to be 2.6 pm/V which is much larger than that predicted from the relationship of

$$r_{33} = \frac{4}{n^4} d_{33} \tag{15}$$

This large apparent coefficients may mainly be due to the piezoelectric response of urea polymers.

Effects of Thermal Annealing on SHG Coefficients. Figure 12 shows the dependence of SH coefficients for the poled sample on thermal annealing at successively higher temperature. All measurements of SHG activity were made at room temperature after the sample film was thermally annealed at given temperature. Each SH coefficient was largely decreased above 60 °C, which is close to the glass transition temperature of PU7.

Conclusion

The effects of drawing and poling on refractive indices and second-order optical nonlinearity have been investigated for uniaxially drawn and poled aliphatic polyurea PU7 films. Polarization reversal is ascribed to the orientation of dipoles driven by external electric field in both the amorphous and crystalline states. Drawing caused the large anisotropy which is evaluated from the change of the refractive indices along three laboratory frame. Increase of draw ratio led to the decrease of the average molecular angle $\overline{\Phi_X}$ and the increase of $\overline{\Phi_Y}$ and $\overline{\Phi_Z}$. For films drawn to the higher ratio of 2.0 and 2.5, Kleinman symmetry was not satisfied: $d_{31} \neq d_{15}$ and $d_{32} \neq d_{24}$. Increase of draw ratio gave rise to the large increase of the tensor components d_{33} and d_{31}, the moderate increase of d_{24}, and the gradual decrease of d_{15} and d_{32}. It is noted that the tensor component d_{31} is the largest at the draw ratio of 2.5. This result suggests that the urea dipoles aligns along the oriented chain direction by drawing. A large linear dependence of electrooptic response on electric field is ascribed to the linear electrooptic (Pockels) effect as well as the piezoelectric response. Second-order nonlinearity was largely depressed above the glass transition temperature of PU7.

Acknowledgment. This work is in part supported by Grants-in-Aid for Scientific Research on Priority Areas, No. 08236223 and 09222214 and for Scientific Research No. 10650888 from the Ministry of Education, Science, Culture, and Sports.

References and Notes

(1) Bergman, J. G.; McFee, J. H.; Crane G. R. *Appl. Phys. Lett.* **1971**, *18*, 203.
(2) McFee, J. H.; Bergman, J. G.; Crane G. R. *Ferroelectrics* 1972, *3*, 305.
(3) Sato, H.; Gamo, H. *Jpn. J. Appl. Phys.* **1986**, *25*, L990.
(4) Wicker, A.; Berge, B.; Lajzerowicz, J.; Legrand, J. F. *J. Appl. Phys.* **1989**, *66*, 342.
(5) Hill, J. R.; Dunn, P. L.; Davies, G. J.; Oliver, S. N.; Patelis, P.; Rush, J. D. *Electron. Lett.* **1987**, *23*, 700.
(6) Tsutsumi, N.; Ono, T.; Kiyotsukuri, T. *Macromolecules* **1993**, *26*, 5447.
(7) Tsutsumi, N.; Fujii, I.; Ueda, Y.; Kiyotsukuri, T. *Macromolecules* **1995**, *28*, 950.
(8) Lee, J. W.; Takase, Y.; Newman, B. A.; Scheinbeim, J. I. *J. Polym. Sci., Part B: Polym. Phys.* **1991**, *29*, 273.
(9) Lee, J. W.; Takase, Y.; Newman, B. A.; Scheinbeim, J. I. *J. Polym. Sci., Part B: Polym. Phys.* **1991**, *29*, 279.
(10) Tsutsumi, N.; Mizutani, T.; Sakai, W. *Macromolecules* **1997**, *30*, 1637.
(11) Tsutsumi, N.; Mizutani, T.; Sakai, W.; Watanabe T.; Miyata, S. *J. Chem. Phys.* **1998**, *108*, 9839.
(12) Bauer, F. *Ferroelectrics* **1983**, *49*, 231.
(13) Bur A. J.; Roth, S. C. *Preparation of Thin Film Polyvinylidene Fluoride Shock Wave Pressure Transducers*; Interagency Report 87-3680, NTIS PB881560070; U.S. National Bureau of Standards: Washington, DC, 1987.
(14) Teng C. C.; Man, H. T. *Appl. Phys. Lett.* **1990**, *56*, 1734.
(15) Maker, P. D.; Terhune, R. W.; Nisenoff, M.; Savage, C. M. *Phys. Rev. Lett.* **1962**, *8*, 21.
(16) Jerphagnon J.; Kurtz, S. K. *J. Appl. Phys.* **1970**, *40*, 1667.
(17) Desper C. R.; Stein, R. S. *J. Appl. Phys.* **1966**, *37*, 3990.
(18) Takahara, H.; Nomura, S.; Kawai, H.; Yamaguchi, Y.; Okazaki, K.; Fukushima, A. *J. Polym. Sci. Polym. Chem.* **1968**, *A-2*, *6*, 197.
(19) van Krevelen, D. W. *Properties of Polymers*, 3rd ed.; Elsevier: Amsterdam, 1990; Chapter 10, pp 298−307. ($n_{\parallel} - n_{\perp}$) is estimated from the data for Nylon 6 and Nylon 66.
(20) Prasad P. N.; Williams, D. J. *Introduction to Nonlinear Optical Effects in Molecules and Polymers*; Wiley-Interscience: New York, 1991; Chapter 4, pp 66−73.
(21) Watanabe, T.; Kim, J.; Miyata, S. In *Poled Polymers and their Applications to SHG and EO Devices*; Miyata, S., Sasabe, H. Gordon and Breach Science: Amsterdam, The Netherlands, 1997; Chapter 5a, pp 109−130.

MA981704K